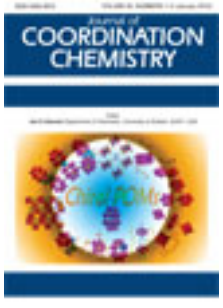

Journal of Coordination Chemistry
Publication details, including instructions for authors and subscription information:
http://www.tandfonline.com/loi/gcoo20

Syntheses of phenoxo-bridged Zn(II) and metallamacrocyclic Hg(II) complexes of organochalcogen (Se, Te) substituted Schiff-bases: structure and DNA-binding studies of Zn(II) complexes

A.K. Asatkar [a], S. Nair [a], V.K. Verma [a], C.S. Verma [a], T.A. Jain [a], R. Singh [b], S.K. Gupta [c] & R.J. Butcher [d]

[a] Department of Chemistry, Disha Institute of Management and Technology, Raipur 492101, Chhattisgarh, India

[b] ER&IPR, Defence Research and Development Organization, New Delhi 110105, India

[c] School of Studies in Chemistry, Jiwaji University, Gwalior 474011, India

[d] Department of Inorganic and Structural Chemistry, Howard University, Washington, DC 20059, USA

Published online: 06 Dec 2011.

To cite this article: A.K. Asatkar, S. Nair, V.K. Verma, C.S. Verma, T.A. Jain, R. Singh, S.K. Gupta & R.J. Butcher (2012) Syntheses of phenoxo-bridged Zn(II) and metallamacrocyclic Hg(II) complexes of organochalcogen (Se, Te) substituted Schiff-bases: structure and DNA-binding studies of Zn(II) complexes, Journal of Coordination Chemistry, 65:1, 28-47, DOI: 10.1080/00958972.2011.639874

To link to this article: http://dx.doi.org/10.1080/00958972.2011.639874

Journal of Coordination Chemistry
Vol. 65, No. 1, 10 January 2012, 28–47

Syntheses of phenoxo-bridged Zn(II) and metallamacrocyclic Hg(II) complexes of organochalcogen (Se, Te) substituted Schiff-bases: structure and DNA-binding studies of Zn(II) complexes

A.K. ASATKAR†, S. NAIR†, V.K. VERMA*†, C.S. VERMA†, T.A. JAIN†, R. SINGH‡, S.K. GUPTA§ and R.J. BUTCHER¶

†Department of Chemistry, Disha Institute of Management and Technology, Raipur 492101, Chhattisgarh, India
‡ER&IPR, Defence Research and Development Organization, New Delhi 110105, India
§School of Studies in Chemistry, Jiwaji University, Gwalior 474011, India
¶Department of Inorganic and Structural Chemistry, Howard University, Washington, DC 20059, USA

(*Received 7 July 2011; in final form 11 October 2011*)

The coordination of organochalcogen (especially Se and Te) substituted Schiff-bases **L^{1}H**, **L^{2}H**, **L^{3}H**, and **L^{4}H** toward Zn(II) and Hg(II) has been studied. Reactions of these ligands with $ZnCl_2$ in 1:1 molar ratio gave binuclear complexes [{2-[PhX$(CH_2)_n$N = C(Ph)]-6-[PhCO]-4-MeC_6H_2O}$_2Zn_2Cl_2$] (where X = Se, $n = 2$ (**1**); X = Se, $n = 3$ (**2**); X = Te, $n = 2$ (**3**); and X = Te, $n = 3$ (**4**)) with partial hydrolytic cleavage of proligands. In these complexes, two partially hydrolyzed ligand fragments coordinate tridentate (*NOO*) with two Zn's. Reaction of $HgBr_2$ with **L^{1}H** and **L^{2}H** in 1:1 molar ratio gave monometallic complexes [C_6H_2(4-Me)(OH)[2,6-{C(Ph) = N$(CH_2)_n$Se(Ph)}$_2$HgBr$_2$]] ($n = 2$ (**5**) or 3 (**6**)) and under similar conditions with **L^{3}H** and **L^{4}H** gave bimetallic complexes [C_6H_2(4-Me)(OH)[2,6-{C(Ph) = N$(CH_2)_n$Te(Ph)}$_2$Hg$_2$Br$_4$]] ($n = 2$ (**7**) or 3 (**8**)) in which the ligands coordinate with metal through selenium or tellurium, leaving the imino nitrogen and phenolic oxygen uncoordinated. The proligands **L^{1}H**, **L^{2}H** give 14- or 16-membered metallamacrocycles through Se–Hg–Se linkages and **L^{3}H**, **L^{4}H** give 16- or 18-membered metallamacrocycles through Te–Hg–Br–Hg–Te linkages. All the complexes were characterized by elemental analyses, ESIMS, FTIR, multinuclear NMR, UV-Vis, and conductance measurements. The redox properties of the complexes were investigated by cyclic voltammetry (CV). Complexes **1**–**4** exhibited ligand-centered irreversible oxidation processes. Complexes **5** and **6** showed metal-centered quasi-reversible single electron transfer, whereas dinuclear complexes **7** and **8** displayed two quasi-reversible, one-electron transfer steps. A single-crystal X-ray structure determination of **1** showed that the coordination unit is centrosymmetric with Zn(II) in square-pyramidal coordination geometry and the two square pyramids sharing an edge. The Zn ⋯ Zn separation is 3.232 Å. The DNA-binding properties of **1** and **3** with calf thymus DNA were explored by a spectrophotometric method and CV.

Keywords: Organoselenium/tellurium; Schiff-base; Zn(II) and Hg(II) complexes; X-ray structure; Cyclic voltammetry; DNA-binding

*Corresponding author. Email: verma_vinay2002@rediffmail.com

ISSN 0095-8972 print/ISSN 1029-0389 online
http://dx.doi.org/10.1080/00958972.2011.639874

1. Introduction

Recent advances in heavier organochalcogen chemistry have been driven by the potential applications of their compounds in organic synthesis (especially in functional group manipulations and asymmetric synthesis) [1–6], ligand chemistry [7–10], biochemistry [11–14], and material science [15–18]. The coordination chemistry of organochalcogen substituted ligands is an area of growing interest [8–10, 19–21] due to potential applications of their mono/multimetallic complexes as single source molecular precursors for generation of monodispersed binary and ternary metal chalcogenide nano materials by chemical vapor deposition (CVD) [22–25], metalloenzymes containing multimetallic centers as active sites for a number of catalytic reactions [26, 27], and so forth. Many important technological applications, e.g., light emitting diodes [28, 29], solar cells [30, 31], and other electronic devices [32, 33] that have been found for a number of metal chalcogenides with their remarkable diversity in their structure and properties have been the driving force of the incredible expansion of these areas of research. As a part of our ongoing research into design and synthesis of novel chalcogen bearing hybrid ligands, we have very recently reported [34, 35] the synthesis of phenol-based Schiff bases $[C_6H_2(OH)(4\text{-}CH_3)\{(PhC{=}N(CH_2)_nXPh)\}_2]$ ($\mathbf{L^1H}$, X = Se, $n = 2$; $\mathbf{L^2H}$, X = Se, $n = 3$; $\mathbf{L^3H}$, X = Te, $n = 2$; $\mathbf{L^4H}$, X = Te, $n = 3$) and their Cu(II) complexes. Herein, we report the synthesis and characterization of Zn(II) and Hg(II) complexes with the proligands $\mathbf{L^1H}$, $\mathbf{L^2H}$, $\mathbf{L^3H}$, and $\mathbf{L^4H}$. A comparative study of Zn(II) complexes of selenium bearing ligands (**1**, **2**), thus formed, with those of their tellurium analogs (**3**, **4**) is also reported. The structures of $\mathbf{L^1H}$, $\mathbf{L^2H}$, $\mathbf{L^3H}$, and $\mathbf{L^4H}$ and their Zn(II) and Hg(II) complexes are shown below.

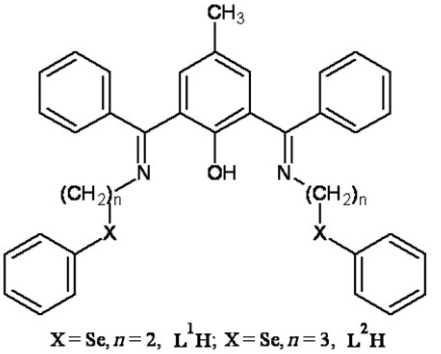

X = Se, $n = 2$, $\mathbf{L^1H}$; X = Se, $n = 3$, $\mathbf{L^2H}$
X = Te, $n = 2$, $\mathbf{L^3H}$; X = Te, $n = 3$, $\mathbf{L^4H}$

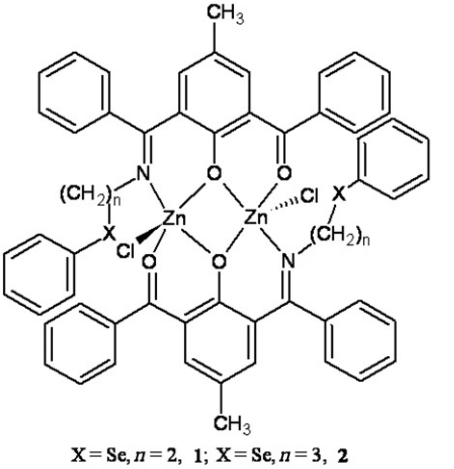

X = Se, $n = 2$, 1; X = Se, $n = 3$, 2
X = Te, $n = 2$, 3; X = Te, $n = 3$, 4

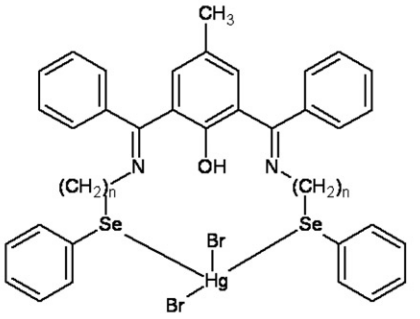

$n = 2$, **5**; $n = 3$, **6**

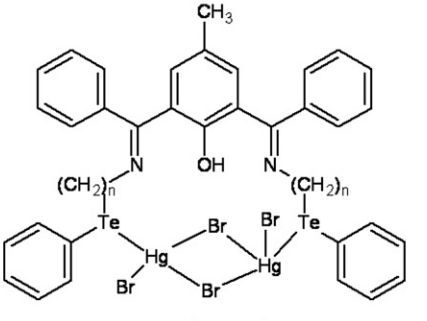

$n = 2$, **7**; $n = 3$, **8**

2. Experimental

2.1. *Reagents*

All the chemicals used were of reagent grade. Solvents were purified by standard methods [36] and freshly distilled prior to use. All the reactions were performed under argon. Proligands $\mathbf{L^1H}$, $\mathbf{L^2H}$, $\mathbf{L^3H}$, and $\mathbf{L^4H}$ were synthesized following the reported methods [34, 35]. Calf thymus (CT) DNA was obtained from Sigma and used as received. The sodium salt of CT-DNA was stored at 277 K.

2.2. *Physical measurements*

Melting points of the compounds in the capillary tubes were recorded and are reported. C, H, and N analyses were carried out on a Carlo-Erba Model DP 200 analyzer. Quantitative estimation of Zn, Hg, Se, and Te were carried out on a Varian Atomic Absorption Spectrophotometer AA 240 FS. The halogens were estimated titrimetrically by Volhard's method. Conductance values were measured using a Century CC-601 digital conductivity meter in acetonitrile at 273 K.

Electrospray ion mass spectra (ESIMS) were recorded on a WATERS-HAB 213 triple quadrupole mass spectrometer. The ESI capillary was set at 3.5 kV and the cone voltage was 40 V. Infrared spectra were recorded from 4000 to 400 cm^{-1} by a Shimadzu IR Prestige-21 FT spectrophotometer on a KBr disc. Electronic spectra were obtained by use of a Perkin Elmer Lambda 35 UV-VIS spectrophotometer. The ^1H and $^{13}C\{^1H\}$ NMR spectra were recorded on a Bruker AMX-400 FT NMR spectrophotometer in $CDCl_3$; the chemical shifts were recorded relative to $SiMe_4$. The $^{77}Se\{^1H\}$ and $^{125}Te\{^1H\}$ NMR spectra were recorded on the same instrument using Ph_2Se_2 and Ph_2Te_2 as external reference and values are reported relative to Me_2Se and Me_2Te (δ 0 ppm).

2.3. *Preparation of zinc and mercury complexes*

2.3.1. Synthesis of zinc complexes 1–4. 10 mL methanolic solution of $ZnCl_2$ (0.136 g, 1.00 mmol) was added dropwise to a 50 mL degassed methanolic solution of proligand $\mathbf{L^1H}$ (0.680 g, 1.00 mmol)/$\mathbf{L^2H}$ (0.708 g, 1.00 mmol)/$\mathbf{L^3H}$ (0.778 g, 1.00 mmol)/$\mathbf{L^4H}$ (0.806 g, 1.00 mmol) under argon with vigorous stirring at room temperature. Precipitation of yellow solid started after ~10 minutes of mixing of the reactants. The progress of reaction was monitored by TLC. After stirring the reaction mixture for 12 h, the precipitated solid was filtered and washed thoroughly with methanol to remove excess unreacted metal salt or ligand. Products were dried under vacuum. The characteristics of the products are given below.

2.3.1.1. *[{2-[PhSeCH$_2$CH$_2$N=C(Ph)]-6-[PhCO]-4-MeC$_6$H$_2$O}$_2$Zn$_2$Cl$_2$] (**1**).* Color and state: yellow powder; yield: 72%; m.p.: 225°C. Anal. Calcd for $C_{58}H_{48}N_2O_4Se_2Zn_2Cl_2$ (%): C, 58.21; H, 4.04; N, 2.34; Zn, 10.93; Se, 13.20; Cl, 5.93. Found (%): C, 57.66; H, 4.42; N, 2.51; Zn, 10.21; Se, 13.95; Cl, 5.71. Positive ESIMS: *m/z* 1159 [**1**-{Cl}]$^+$, 1097, 1061, 500. FTIR (KBr disc, cm^{-1}): 1610 ν(C=O), 1582 ν(C=C), 1532 ν(C=N), 1248 ν(C–O), 556 ν(Zn–N), 503 ν(Zn–$O_{phenolic}$), 407 ν(Zn–$O_{benzoylic}$). ^{1}H NMR ($CDCl_3$, δ, ppm, TMS): 7.97–6.91 (m, 34H, C_6H_5 and C_6H_2), 3.71 (t, 4H, N–CH_2), 3.06 (t, 4H, Se–CH_2), 2.21 (s, 6H, CH_3). ^{13}C {^{1}H} NMR ($CDCl_3$, δ, ppm, TMS): 203 (C=O), 179 (C=N), 169 (C–O), 145–123 (Ar–C), 56 (N–CH_2), 26 (Se–CH_2), 20 (CH_3). ^{77}Se{^{1}H} NMR ($CDCl_3$, δ, ppm, Me_2Se): 290. UV-Vis (λ_{max} nm, ε (mol L^{-1})$^{-1}$ cm^{-1}, CH_3CN): 250 (15,427), 344 (3062), 416 (2031). Λ_M (10^{-3} mol L^{-1}, CH_3CN, 298 K): 20 Ω^{-1} cm^2 mol^{-1}.

2.3.1.2. *[{2-[PhSeCH$_2$CH$_2$CH$_2$N=C(Ph)]-6-[PhCO]-4-MeC$_6$H$_2$O}$_2$Zn$_2$Cl$_2$] (**2**).* Color and state: yellow powder; yield: 76%; m.p.: 229°C. Anal. Calcd for $C_{60}H_{52}N_2O_4Se_2Zn_2Cl_2$ (%): C, 58.84; H, 4.28; N, 2.29; Zn, 10.68; Se, 12.89; Cl, 5.79. Found (%): C, 58.47; H, 4.25; N, 2.96; Zn, 10.07; Se, 13.64; Cl, 5.43. Positive ESIMS: *m/z* 1187 [**2**-{Cl}]$^+$, 1125, 1089, 514. FTIR (KBr disc, cm^{-1}): 1611 ν(C=O), 1584 ν(C=C), 1531 ν(C=N), 1247 ν(C–O), 556 ν(Zn–N), 503 ν(Zn–$O_{phenolic}$), 413 ν(Zn–$O_{benzoylic}$). ^{1}H NMR ($CDCl_3$, δ, ppm): 8.02–6.99 (m, 34H, C_6H_5 and C_6H_2), 3.51 (t, 4H, N–CH_2), 3.01 (t, 4H, Se–CH_2), 2.10 (q, 4H, mid-CH_2 (CH_2 between N–CH_2 and Se–CH_2)), 2.13 (s, 6H, CH_3). ^{13}C{^{1}H} NMR ($CDCl_3$, δ, ppm, TMS): 203 (C=O), 178 (C=N), 168 (C–O), 145–123 (Ar–C), 55 (N–CH_2), 31 (mid-CH_2), 24 (Se–CH_2), 20 (CH_3). ^{77}Se{^{1}H} NMR ($CDCl_3$, δ, ppm, Me_2Se): 293. UV-Vis (λ_{max} nm, ε (mol L^{-1})$^{-1}$ cm^{-1}, CH_3CN): 248 (15,638), 345 (3126), 412 (2431). Λ_M (10^{-3} mol L^{-1}, CH_3CN, 298 K): 22 Ω^{-1} cm^2 mol^{-1}.

2.3.1.3. *[{2-[PhTeCH$_2$CH$_2$N=C(Ph)]-6-[PhCO]-4-MeC$_6$H$_2$O}$_2$Zn$_2$Cl$_2$] (**3**).* Color and state: yellow powder; yield: 68%; m.p.: 190°C. Anal. Calcd for $C_{58}H_{48}N_2O_4Te_2Zn_2Cl_2$ (%): C, 53.84; H, 3.74; N, 2.16; Zn, 10.11; Te, 19.72; Cl, 5.48. Found (%): C, 54.01; H, 3.86; N, 2.42; Zn, 10.26; Te, 19.87; Cl, 5.39. Positive ESIMS: *m/z* 1294 [**3**]$^+$, 1259, 1097, 550. FTIR (KBr disc, cm^{-1}): 1614 ν(C=O), 1591 ν(C=C), 1537 ν(C=N), 1244 ν(C–O), 555 ν(Zn–N), 491 ν(Zn–$O_{phenolic}$), 410 ν(Zn–$O_{benzoylic}$). ^{1}H NMR ($CDCl_3$, δ, ppm, TMS): 7.97–6.75 (m, 34H, C_6H_5 and C_6H_2), 3.43 (t, 4H, N–CH_2), 3.01 (t, 4H, Te–CH_2), 2.11 (s, 6H, CH_3). ^{13}C {^{1}H} NMR ($CDCl_3$, δ, ppm, TMS): 204 (C=O), 177 (C=N), 169 (C–O), 145–123 (Ar–C), 57 (N–CH_2), 20 (Te–CH_2),

10 (CH_3). $^{125}Te\{^1H\}$ NMR ($CDCl_3$, δ, ppm, Me_2Te): 469. UV-Vis (λ_{max} nm, ε $(mol\,L^{-1})^{-1}\,cm^{-1}$, CH_3CN): 297 (1530), 345 (2610), 394 (2960). Λ_M ($10^{-3}\,mol\,L^{-1}$, CH_3CN, 298 K): $27\,\Omega^{-1}\,cm^2\,mol^{-1}$.

2.3.1.4. *[{2-[PhTeCH$_2$CH$_2$CH$_2$N=C(Ph)]-6-[PhCO]-4-MeC$_6$H$_2$O}$_2$Zn$_2$Cl$_2$] (**4**)*. Color and state: yellow powder; yield: 71%; m.p.: 224°C. Anal. Calcd for $C_{60}H_{52}N_2O_4Te_2Zn_2Cl_2$ (%): C, 54.51; H, 3.96; N, 2.12; Zn, 9.90; Te, 19.30; Cl, 5.36. Found (%): C, 54.39; H, 4.12; N, 2.32; Zn, 10.03; Te, 19.47; Cl, 5.46. Positive ESIMS: *m/z* 1322 $[4]^+$, 1295, 1259, 1123, 564. FT IR (KBr disc, cm^{-1}): 1614 ν(C=O), 1591 ν(C=C), 1537 ν(C=N), 1246 ν(C–O), 555 ν(Zn–N), 491 ν(Zn–$O_{phenolic}$), 410 ν(Zn–$O_{benzoylic}$). ^1H NMR ($CDCl_3$, δ, ppm): 7.78–6.82 (m, 34H, C_6H_5 and C_6H_2), 3.64 (t, 4H, N–CH_2), 2.83 (t, 4H, Te–CH_2), 2.41 (q, 4H, mid-CH_2 (CH_2 between N–CH_2 and Te–CH_2)), 2.10 (s, 6H, CH_3). $^{13}C\{^1H\}$ NMR ($CDCl_3$, δ, ppm, TMS): 204 (C=O), 177 (C=N), 169 (C–O), 145–123 (Ar–C), 56 (N–CH_2), 34 (mid-CH_2), 32 (Te–CH_2), 20 (CH_3). $^{125}Te\{^1H\}$ NMR ($CDCl_3$, δ, ppm, Me_2Te): 477. UV-Vis (λ_{max} nm, ε $(mol\,L^{-1})^{-1}\,cm^{-1}$, CH_3CN): 292 (1320), 342 (1840), 404 (930). Λ_M ($10^{-3}\,mol\,L^{-1}$, CH_3CN, 298 K): $19\,\Omega^{-1}\,cm^2\,mol^{-1}$.

2.3.2. Synthesis of mercury complexes 5–8. A solution of **L^{1}H** (0.680 g, 1.00 mmol)/ **L^{2}H** (0.708 g, 1.00 mmol)/**L^{3}H** (0.778 g, 1.00 mmol)/**L^{4}H** (0.806 g, 1.00 mmol) in 30 mL dry acetonitrile was added dropwise to a solution of mercury bromide (0.360 g, 1.00 mmol in 15 mL acetonitrile) with stirring over the period of 1 h. As the ligand solutions were added to the mercury bromide, initially a precipitate appeared, which started to dissolve within 10 min. It was stirred continuously for 12 h and concentrated under vacuum to obtain yellow powder. The products were recrystallized with diethylether. The characteristics of the products are given below.

2.3.2.1. *[{2,6-[PhSeCH$_2$CH$_2$N=C(Ph)]$_2$-4-MeC$_6$H$_2$(OH)}HgBr$_2$] (**5**)*. Color and state: yellow powder; yield: 71%; m.p.: 65°C. Anal. Calcd for $C_{37}H_{34}N_2OSe_2HgBr_2$ (%): Hg, 19.27; Se, 15.17; Br, 15.35. Found (%): Hg, 20.15; Se, 15.63; Br, 15.03. Positive ESIMS: *m/z* 1046 $[\mathbf{5}]^+$, 883, 805, 683, 500. FTIR (KBr disc, cm^{-1}): 3429 b ν(O–H), 1601 ν(C=N), 1572 ν(C=C), 1250 ν(C–O). ^1H NMR ($CDCl_3$, δ, ppm, TMS): 15.60 (s, 1H, OH), 7.90–7.00 (m, 22H, C_6H_5 and C_6H_2), 3.60 (t, 4H, N–CH_2), 2.91 (t, 4H, Se–CH_2), 2.17 (s, 3H, CH_3). $^{13}C\{^1H\}$ NMR ($CDCl_3$, δ, ppm, TMS): 177 (C=N), 159 (C–O), 140–118 (Ar–C), 51 (N–CH_2), 23 (Se–CH_2), 20 (CH_3). $^{77}Se\{^1H\}$ NMR ($CDCl_3$, δ, ppm, dimethylselenide): 247. UV-Vis (λ_{max} nm, ε $(mol\,L^{-1})^{-1}\,cm^{-1}$, CH_3CN): 255 (14,381), 329 (3289), 453 (2071). Λ_M ($10^{-3}\,mol\,L^{-1}$, CH_3CN, 298 K): $19\,\Omega^{-1}\,cm^2\,mol^{-1}$.

2.3.2.2. *[{2,6-[PhSeCH$_2$CH$_2$CH$_2$N=C(Ph)]$_2$-4-MeC$_6$H$_2$(OH)}HgBr$_2$] (**6**)*. Color and state: yellow powder; yield (%): 68; m.p.: 75°C. Anal. Calcd for $C_{39}H_{38}N_2OSe_2HgBr_2$ (%): Hg, 18.76; Se, 14.77; Br, 14.95. Found (%): Hg, 19.09; Se, 14.27; Br, 15.19. Positive ESIMS: *m/z* 1074 $[\mathbf{6}]^+$, 1047, 986, 711, 514. FTIR (KBr disc, cm^{-1}): 3451 b ν(O–H), 1600 ν(C=N), 1577 ν(C=C), 1268 ν(C–O). ^1H NMR ($CDCl_3$, δ, ppm, TMS): 16.20 (s, 1H, OH), 7.90–6.70 (m, 22H, C_6H_5 and C_6H_2), 3.35 (t, 4H, N–CH_2), 2.80 (t, 4H, Se–CH_2), 2.16 (q, 4H, mid-CH_2 (CH_2 between N–CH_2 and Se–CH_2)), 2.29 (s, 3H, CH_3). $^{13}C\{^1H\}$ NMR ($CDCl_3$, δ, ppm, TMS): 175 (C=N), 159 (C–O), 145–1180 (Ar–C), 51 (N–CH_2), 30 (mid-CH_2), 22 (Se–CH_2), 20 (CH_3). $^{77}Se\{^1H\}$ NMR

($CDCl_3$, δ, ppm, dimethylselenide): 249. UV-Vis (λ_{max} nm, ε $(mol\,L^{-1})^{-1}\,cm^{-1}$, CH_3CN): 257 (15,132), 335 (926), 449 (2259). Λ_M (10^{-3} mol L^{-1}, CH_3CN, 298 K): 21 $\Omega^{-1}\,cm^2\,mol^{-1}$.

2.3.2.3. *[{2,6-[PhTeCH$_2$CH$_2$N=C(Ph)]$_2$-4-MeC$_6$H$_2$(OH)}Hg$_2$Br$_4$] (**7**)*. Color and state: yellow powder; yield: 49%; m.p.: 109°C. Anal. Calcd for $C_{37}H_{34}N_2OTe_2Hg_2Br_4$ (%): Hg, 26.77; Te, 17.03; Br, 21.33. Found (%): Hg, 26.89; Te, 17.62; Br, 21.79. Positive ESIMS: *m/z* 1498 [**7**]$^+$, 1328, 779, 550. FTIR (KBr disc, cm^{-1}): 3423 b ν(O–H), 1610 ν(C=N), 1590 ν(C=C), 1251 ν(C–O). ^{1}H NMR ($CDCl_3$, δ, ppm, TMS): 16.01 (s, 1H, OH), 7.90–7.00 (m, 22H, C_6H_5 and C_6H_2), 3.63 (t, 4H, N–CH_2), 3.00 (t, 4H, Te–CH_2), 2.15 (s, 3H, CH_3). ^{13}C{^{1}H} NMR ($CDCl_3$, δ, ppm, TMS): 177 (C=N), 157 (C–O), 138–127 (Ar–C), 51 (N–CH_2), 21 (Te–CH_2), 20 (CH_3). ^{125}Te{^{1}H} NMR ($CDCl_3$, δ, ppm, dimethyltelluride): 365. UV-Vis (λ_{max} nm, ε $(mol\,L^{-1})^{-1}\,cm^{-1}$, CH_3CN): 253 (8036), 339 (3908), 452 (1864). Λ_M (10^{-3} mol L^{-1}, CH_3CN, 298 K): 35 $\Omega^{-1}\,cm^2\,mol^{-1}$.

2.3.2.4. *[{2,6-[PhTeCH$_2$CH$_2$CH$_2$N=C(Ph)]$_2$-4-MeC$_6$H$_2$(OH)}Hg$_2$Br$_4$] (**8**)*. Color and state: yellow powder; yield: 48%; m.p.: 104°C. Anal. Calcd for $C_{39}H_{38}N_2OTe_2Hg_2Br_4$ (%): Hg, 26.28; Te, 16.72; Br, 20.93. Found (%): Hg, 26.91; Te, 17.01; Br, 21.20. Positive ESIMS: *m/z* 1370 [**8**-{Br_2}]$^+$, 1162, 807, 564. FTIR (KBr disc, cm^{-1}): 3431 b ν(O–H), 1609 ν(C=N), 1597 ν(C=C), 1250 ν(C–O). ^{1}H NMR ($CDCl_3$, δ, ppm, TMS): 16.26 (s, 1H, OH), 7.90–6.70 (m, 22H, C_6H_5 and C_6H_2), 3.31 (t, 4H, N–CH_2), 3.04 (t, 4H, Te–CH_2), 2.01 (q, 4H, mid-CH_2 (CH_2 between N–CH_2 and Te–CH_2)), 2.10 (s, 3H, CH_3). ^{13}C{^{1}H} NMR ($CDCl_3$, δ, ppm, TMS): 175 (C=N), 161 (C–O), 139–125 (Ar–C), 52 (N–CH_2), 31 (mid-CH_2(CH_2 between N–CH_2 and Te–CH_2)), 21 (Te–CH_2), 17 (CH_3). ^{125}Te{^{1}H} NMR ($CDCl_3$, δ, ppm, dimethyltelluride): 393. UV-Vis (λ_{max} nm, ε $(mol\,L^{-1})^{-1}\,cm^{-1}$, CH_3CN): 254 (2470), 345 (450), 435 (130). Λ_M (10^{-3} mol L^{-1}, CH_3CN, 298 K): 83 $\Omega^{-1}\,cm^2\,mol^{-1}$.

2.4. *X-ray structure determination*

Attempts were made to grow single crystals of all the isolated complexes. However, single crystals of only **1** could be obtained by slow evaporation of solvent from its solution in chloroform–hexane system. X-ray data were collected on an Oxford Diffraction Xcalibur Ruby Gemini diffractometer with Cu-Kα radiation ($\lambda = 1.54178$ Å) at 295 K. The structure solution and refinements were made by SHELXS-97 and SHELXL-97 [37]. Absorption corrections were made by multi-scan *CrysAlis PRO* [38]. Non-hydrogen atoms were anisotropic and hydrogen positions were included in the riding mode. The SHELXLTL program [37] was used to prepare molecular graphics. Data collection parameters are given in table 1. Selected bond lengths and angles are listed in table 2.

2.5. *Cyclic voltammetry*

Cyclic voltammetric (CV) measurements were carried out with the advanced electrochemical system, BASi Epsilon 828 and PARSTAT 2253 instruments equipped with a three-electrode system. The micro-cell model BAS C3 Cell Stand and model KO264

Table 1. Crystal data and structure refinement for **1**.

Empirical formula	$C_{58}H_{48}Cl_2N_2O_4Se_2Zn_2$
Formula weight	1196.54
Temperature (K)	295(2)
Wavelength (Å)	1.54178
Crystal system	Monoclinic
Space group	$C2/c$
Unit cell dimensions (Å, °)	
a	21.6875(5)
b	14.1540(3)
c	18.6267(6)
α	90
β	106.988(3)
γ	90
Volume (Å^3), Z	5468.3(2), 4
Calculated density (Mg m^{-3})	1.453
Absorption coefficient (mm^{-1})	3.867
F(000)	2416
Crystal size (mm^3)	$0.42 \times 0.36 \times 0.25$
θ range for data collection (°)	4.85–77.72
Index ranges	$-18 \le h \le 27$; $-17 \le k \le 17$; $-23 \le l \le 23$
Reflections collected	13,279
Independent reflections	5720 [R(int) = 0.0397]
Completeness to $\theta = 67.50$ (%)	99.5
Absorption correction	Semi-empirical from equivalents
Max. and min. transmission	1.00000 and 0.35630
Refinement method	Full-matrix least-squares on F^2
Data/restraints/parameters	5720/0/269
Goodness-of-fit on F^2	1.064
Final R indices [$I > 2\sigma(I)$]	$R_1 = 0.0737$, $wR_2 = 0.2027$
R indices (all data)	$R_1 = 0.0842$, $wR_2 = 0.2116$
Largest difference peak and hole (e Å^{-3})	1.124 and −0.866

Table 2. Selected bond lengths (Å) and angles (°) for **1** with esd's in parentheses.[a]

Zn–O(1)	1.996(3)
Zn–N(1)	2.065(4)
Zn–O(2)#1	2.097(3)
Zn–O(1)#1	2.108(3)
Zn–Cl	2.224(2)
Se–C(23)	1.948(4)
Se–C(24)	1.914(3)
O(1)–Zn–N(1)	88.60(1)
N(1)–Zn–O(2)#1	90.82(1)
O(2)#1–Zn–O(1)#1	79.41(1)
O(1)–Zn–O(1)#1	76.16(1)
O(1)–Zn–O(2)#1	138.83(1)
N(1)–Zn–O(1)#1	142.06(1)
O(1)–Zn–Cl	116.93(1)
N(1)–Zn–Cl	110.53(1)
O(2)#1–Zn–Cl	101.71(1)
O(1)#1–Zn–Cl	107.34(1)

[a]Symmetry codes: (#1) $-x+1$, $-y+1$, $-z+1$.

consisted of a platinum working electrode, platinum wire as auxiliary electrode, and a non-aqueous Ag/Ag^+ reference electrode with $0.1\,mol\,L^{-1}$ $AgNO_3$ in acetonitrile as filling solution. Tetrabutylammonium perchlorate ($0.1\,mol\,L^{-1}$ solution in CH_3CN) was used as the supporting electrolyte. Cyclic voltammograms with scan speeds of $100–500\,mVs^{-1}$ were run in $10^{-4}\,mol\,L^{-1}$ CH_3CN solution in a nitrogen atmosphere. Under these conditions the ferrocenium/ferrocene (fc^+/fc) couple shows a peak separation of 84 mV.

2.6. *DNA-binding study*

2.6.1. Methodology for DNA-binding analysis using electronic spectra. Experiments involving interaction of the complex with CT-DNA were carried out in doubly distilled water buffer containing $5.0\,mmol\,L^{-1}$ Tris [tris(hydroxymethyl)-aminomethane] and $50\,mmol\,L^{-1}$ NaCl and adjusted to pH 7.2 with hydrochloric acid. Solutions of CT-DNA gave ratios of absorbance at 260 and 280 nm of about 1.8–1.9, indicating that the DNA was free of protein contamination [39].

The DNA concentration per nucleotide was determined spectrophotometrically by employing a molar absorption coefficient of 6600 $(mol\,L^{-1})^{-1}\,cm^{-1}$ at 260 nm after 1 : 100 dilution [40]. The complex was dissolved in 1% DMSO and 99% Tris–HCl buffer ($5.0\,mmol\,L^{-1}$ Tris–HCl, $50\,mmol\,L^{-1}$ NaCl, pH 7.2) at $3.0 \times 10^{-5}\,mol\,L^{-1}$. An absorption titration was performed on $30\,mol\,L^{-1}$ compound by varying the concentration of nucleic acid. While measuring the absorption spectra, an equal amount of CT-DNA was added to both the compound solution and the reference solution to eliminate the absorbance of CT-DNA itself. Titration curves were constructed from the fractional change in absorption intensity as a function of DNA concentration. The intrinsic binding constant, K_b of the complex with CT-DNA was determined according to the following equation [41] through a plot of $[DNA]/(\varepsilon_a–\varepsilon_f)$ *versus* [DNA]:

$$[DNA]/(\varepsilon_a - \varepsilon_f) = [DNA]/(\varepsilon_b - \varepsilon_f) + 1/K_b(\varepsilon_b - \varepsilon_f), \quad (1)$$

where [DNA] is the concentration of DNA in base pairs, the apparent absorption coefficients ε_a, ε_f and ε_b correspond to $A_{observed}/[Zn]$, the extinction coefficient for the free zinc complex and the extinction coefficient for the bound zinc complex, respectively. In plots of $[DNA]/(\varepsilon_a–\varepsilon_f)$ *versus* [DNA], K_b is given by the ratio of the slope to the intercept.

2.6.2. Methodology for DNA-binding analysis using electrochemical technique. CV was carried out on an Advanced Electrochemical System PARSTAT 2253 instrument. All voltammetric experiments were performed in single compartmental cell of volume 10 mL containing a three electrode system comprising a platinum working electrode, platinum wire as auxiliary electrode, and an Ag/AgCl as reference electrode. The supporting electrolyte was $50\,mmol\,L^{-1}$ NaCl, $5\,mmol\,L^{-1}$ Tris, pH 7.2. All samples were purged with nitrogen prior to measurements.

3. Results and discussion

3.1. *Characterization of zinc(II) complexes 1–4*

Zinc complexes **1**–**4**, synthesized by reacting $\mathbf{L^1H}$, $\mathbf{L^2H}$, $\mathbf{L^3H}$, and $\mathbf{L^4H}$, respectively, with $ZnCl_2$ in 1 : 1 molar ratio have composition $[\{2\text{-}[PhX(CH_2)_nN{=}C(Ph)]\text{-}6\text{-}[PhCO]\text{-}4\text{-}MeC_6H_2O\}_2Zn_2Cl_2]$ (where X = Se, $n = 2$ (**1**); X = Se, $n = 3$ (**2**); X = Te, $n = 2$ (**3**); and X = Te, $n = 3$ (**4**)). Analytical data suggest that one arm of the ligand is hydrolyzed at the C=N position and hydrochloric acid is released due to combination of a chloride ion with phenolic proton of the ligands. They are soluble in chloroform, dichloromethane and acetonitrile.

The ESI mass spectra of **1** and **2** show the ion peak corresponding to mass of two molecules of partially hydrolyzed ligands, two zinc atoms plus a chlorine atom, namely $[\{C_6H_2(O)(4\text{-}CH_3)(PhC{=}NCH_2CH_2SePh)(PhC{=}O)\}_2Zn_2Cl]^+$ and $[\{C_6H_2(O)(4\text{-}CH_3)(PhC{=}NCH_2CH_2CH_2SePh)(PhC{=}O)\}_2Zn_2Cl]^+$, which are devoid of a chloride ion from the molecular ion; the parent ion peaks could not be observed. However, **3** and **4** do show their respective molecular ion peak.

In IR spectra of **1**–**4**, ν(C=N) stretching frequencies are shifted to lower frequency by $\sim 60\,cm^{-1}$ with respect to those of the corresponding free proligands. The lower frequency shift in these bands suggests coordination of imino N with Zn(II). In addition to ν(C=N) band, a band appears at $\sim 1610\,cm^{-1}$ in all the spectra. It is attributed to the formation of C=O on hydrolysis of one imine group of the ligand and subsequently its coordination with the metal. Involvement in coordination shift it $\sim 50\,cm^{-1}$ toward the red as compared to 4-methyl-2,6-dibenzoylphenol ($1658\,cm^{-1}$). Further, the disappearance of ν(O–H) vibrational band in the spectra suggests involvement of phenolic proton with chloride of $ZnCl_2$ to form hydrochloric acid and linkage of the phenolic O with Zn(II). Medium to weak intensity bands at $556\,cm^{-1}$, 503–$491\,cm^{-1}$, and 407–$413\,cm^{-1}$ for all the complexes can be assigned to ν(Zn–N), $\nu(Zn\text{–}O_{phenolic})$, and $\nu(Zn\text{–}O_{benzoylic})$, respectively [42]. ^{1}H NMR spectra of the complexes show downfield shifts of N–CH_2 proton signals compared to the free proligands, which suggest coordination of nitrogen with Zn(II). Disappearance of the singlet due to phenolic proton (at $\sim$16 ppm) in the spectra is attributed to its displacement and coordination of phenolic oxygen with metal. However, the positions of the signal due to X–CH_2 protons in the spectra are almost unperturbed, suggesting no involvement of chalcogen in coordination. In $^{13}C\{^1H\}$ NMR spectra of the complexes, the additional signal at 203 ppm is assigned to C=O carbon formed after partial hydrolysis of C=N. Appearance of a single resonance for ^{77}Se and ^{125}Te nuclei almost at the same position as in the free proligands confirms non-involvement of chalcogen with metal. The UV-Vis spectra of complexes in acetonitrile show characteristic bands in the UV region due to $\pi \rightarrow \pi^*$ transitions for phenyl rings (*ca* 250–297 nm) and $\pi \rightarrow \pi^*$ (*ca* 345 nm) transitions. The $\pi \rightarrow \pi^*$ transitions around 345 nm are in accord with extended π-systems between phenolic oxygen to imino nitrogen [43]. The third band around 394–415 nm in the spectra is attributed to $n \rightarrow \pi^*$ transitions. Molar conductance values of complexes in acetonitrile show non-electrolytes and thus eliminate the possibility of ionic products.

Thus, spectroscopic and analytical data of the products suggest that in the complexes each molecule of partially hydrolyzed ligand coordinates tridentate through benzoyl "O", imine "N" and phenolic "O", leaving "Se" and "Te" uncoordinated. The phenolic "O" bridges two Zn(II) ions. Each metal is bonded to chloride and thus, each

Zn(II) adopts square-pyramidal geometry. Square-pyramidal complexes of Zn(II) are well-known in the literature [44–48].

3.2. *Characterization of mercury(II) complexes 5–8*

These complexes have good solubility in chloroform, dichloromethane, methanol, acetonitrile, and acetone. Analytical data of **5**–**8** show good agreement with compositions $C_{37}H_{34}N_2OSe_2HgBr_2$, $C_{39}H_{38}N_2OSe_2HgBr_2$, $C_{37}H_{34}N_2OTe_2Hg_2Br_4$, and $C_{39}H_{38}N_2OTe_2Hg_2Br_4$, respectively. The ESI mass spectra of **5** and **6** show molecular ion peaks corresponding to mass of one ligand, one Hg, and two Br^-'s, suggesting 1 : 1 molar ratio. Replacement of Se by larger Te in the proligands resulted in change in reactivity of the proligands and led to the formation of complexes having 2 : 1 metal to ligand stoichiometry. Recently, Verma *et al.* [35] reported that tellurium in their respective proligands are more sterically hindered than selenium analogs and, hence, both PhTe–$(CH_2)_n$–NH_2 chains lie apart from each other as far as possible, providing space for two metal ions to be accommodated.

In both IR and ^{1}H NMR spectra, bands due to ν(O–H) and ν(C=N) stretching frequencies and OH and N–CH_2 proton signals, respectively, appear at almost the same position as in the free ligands, suggesting no involvement of phenolic "O" and imino "N" in coordination with Hg(II). In ^{1}H NMR spectra slight upfield shifts of the signal due to X–CH_2 protons compared to that of free proligands suggests that in coordination of chalcogen with Hg(II), back donation of electrons from electron rich d^{10} Hg(II) to chalcogen occurs [49, 50]. The $^{13}C\{^1H\}$ NMR data of the complexes corroborate the ^{1}H NMR findings. In ^{77}Se NMR spectra of mercury complexes, signals are at *ca* δ 250 ppm, about 35–40 ppm upfield as compared to those of the free ligands. Similarly ^{125}Te signals in tellurium anologs are shielded by about 84–104 ppm as compared to those of the free proligands. These observations strongly support mercury to selenium/tellurium back donation [51, 52]. The electronic absorption spectra of mercury complexes in acetonitrile show two bands for $\pi \rightarrow \pi^*$ transitions and one band for $n \rightarrow \pi^*$ as expected. The molar conductance values of the complexes in acetonitrile suggest non-ionic nature.

Thus, based on analytical and spectroscopic data of **5** and **6**, it can be inferred that $\mathbf{L^1H}$ and $\mathbf{L^2H}$ coordinate bidentate with a Hg(II) through Se only; the hard donors (N and O) of the proligands remain uncoordinated. The non-ionic nature of the complexes suggests that the metal in each complex is directly attached with two bromides. Hence, in **5** and **6** the metal is tetrahedral. Such binding of the ligands with Hg(II) results in cyclization of the complexes *via* Se–Hg–Se linkage and leads to the formation of 14- and 16-membered monometallic metallamacrocyclic species. Like $\mathbf{L^1H}$ and $\mathbf{L^2H}$, $\mathbf{L^3H}$ and $\mathbf{L^4H}$ also bind with Hg(II) in a similar fashion; however, the complexes have a metal to ligand ratio of 2 : 1, in which each Hg(II) is bonded with one Te and three bromides, of which one is terminal and the other two bridge Hg(II). Similar to **5** and **6**, **7** and **8** also acquire tetrahedral geometry and form 16- and 18-membered bimetallic metallamacrocyclic complexes *via* Te–Hg–Br–Hg–Te linkages.

Mercury(II) being large is a soft acceptor and hence interacts with only soft chalcogens of $\mathbf{L^1H}$, $\mathbf{L^2H}$, $\mathbf{L^3H}$, and $\mathbf{L^4H}$; no hard–soft interaction is observed. Unlike the Zn(II) complexes, Hg(II) complexes do not show hydrolysis at C=N, perhaps because of the soft nature of Hg(II) and hence no affinity toward the phenolic O. Zinc being smaller

in size, prefers to combine with phenolic O and forms stable six-membered rings. Combination of phenolic O with Zn(II) activates its proton to participate with Cl of the metal, resulting in the formation of HCl. The acid thus formed probably catalyzes hydrolysis of one arm of the proligands at C=N position [34, 35].

3.3. *X-ray structure determination*

Single crystals of **1** were obtained by slow evaporation of its solution in chloroform–hexane mixture under hexane vapor. The molecular structure of **1** is shown in figure 1. There are two dimeric molecules per unit cell (Supplementary material) with each having a center of symmetry. The coordination unit consists of two equivalent parts, namely [{C_6H_2(O)(4-CH_3)(PhC=NCH_2CH_2SePh)(PhC=O)}ZnCl], and these two parts combine through bridging phenol. The coordination sphere around each Zn(II) is O_3NCl, namely an imino N, two bridging phenolic oxygen atoms, a benzoylic oxygen, and a terminal Cl^-; O_3N coordination sphere around each Zn(II) forms the basal plane (distorted) of the square pyramid while Cl^- occupies the axial position. Each Zn(II) is displaced from its basal plane toward the Cl^- by 0.68 Å (Supplementary material). The Se of each ligand lies far from Zn, at 5.373 Å. Both square pyramids are *trans* to each other and connected by edge sharing of O1–O1# (figure 2). Zn_2O_2 core is planar and contains a center of symmetry on the same plane inside the core. The separation between the non-bonded metal center (Zn $\cdots$ Zn) is 3.232 Å, slightly larger than that reported for a Zn_2(μ-phenoxide)$_2$ complex [53]. Out of four Zn–$O_{phenoxy}$ distances of the square, two are at 1.996(3) Å and the other two 2.108(3) Å, slightly larger than the reported phenoxy bridged square-pyramidal complexes [53]. However, Zn–N distances

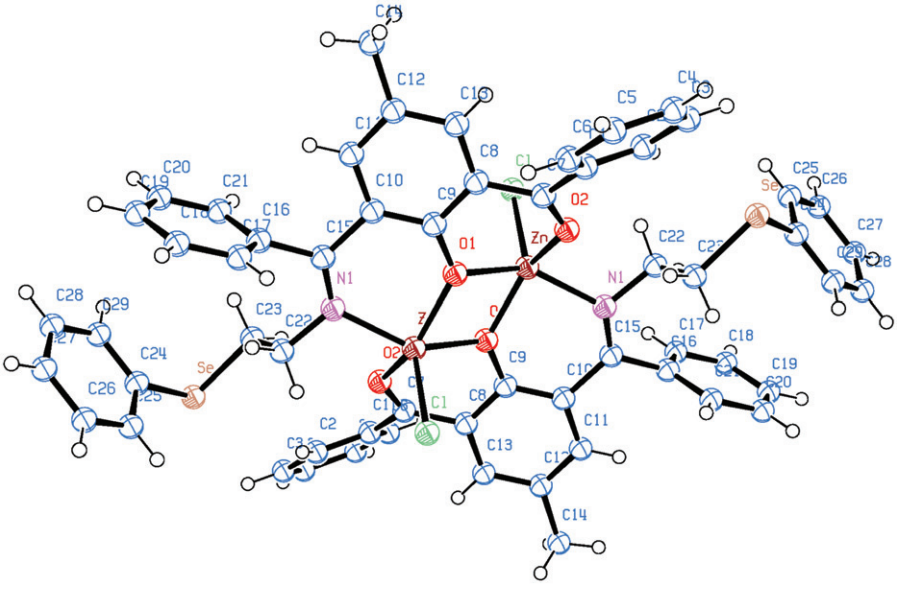

Figure 1. Structure of **1**.

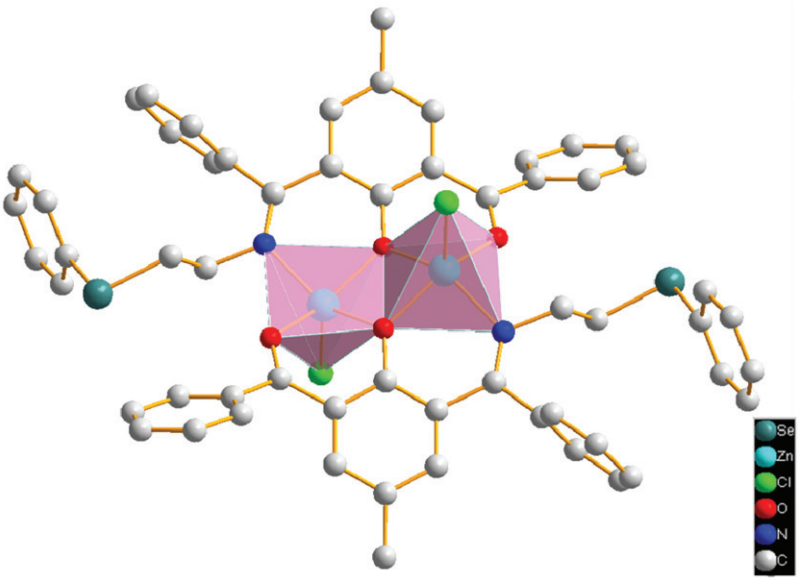

Figure 2. Two square pyramids *trans* to each other. Hydrogen atoms are omitted for clarity.

are 2.065(4) Å. There is no intramolecular secondary interaction in the molecule but various intermolecular non-bonding interactions are present.

3.4. *Cyclic voltammograms of complexes 1–8*

Numerical data from CV studies for **1–4** and **5–8** in 0.1 mmol L^{-1} solution in CH_3CN/0.1 mol L^{-1} $[NBu_4][ClO_4]$ with 100–500 mVs^{-1} scan rates are summarized in tables 3 and 4. The CV data are collected under an argon atmosphere and potentials are reported with reference to Ag/0.1 mol L^{-1} Ag^+. In the cyclic voltammogram of **1–4** (figure 3), the respective electrochemically irreversible oxidation peak is observed at E_{pa} 0.859 V (**1**), 0.835 V (**2**), 0.844 V (**3**), and 0.788 V (**4**). These anodic waves in the CVs of **1–4** are presumed to be proligand centered oxidation and do not display any additional peak when compared with those of their respective proligands under identical conditions. The partial hydrolysis of proligands followed by coordination of hydrolyzed ligand fragments with Zn(II) led to shift of anodic peak potentials to more positive value than those observed for free proligands (E_{pa} 0.778 V (**L^1H**); 0.567 V (**L^2H**) [34]; 0.190 V (**L^3H**); and 0.558 V (**L^4H**) [35]). The observed shifts in oxidation potentials in **3** and **4** compared with tellurium-bearing ligands are much higher than the shift in **1** and **2** compared with selenium analogs. These observations suggest that tellurium bearing ligands in **3** and **4** are more hindered than those of selenium bearing ligands in **1** and **2**, consistent with X-ray observations.

The cyclic voltammograms of **5** and **6** (figure 4) display one quasi-reversible wave at $E^{\circ\prime}$ −0.263 V with E_{pc} −0.482 V, E_{pa} −0.044 V for **5** and $E^{\circ\prime}$ −0.278 V with E_{pc} −0.521 V, E_{pa} −0.036 V for **6** *versus* Ag/Ag^+. These are attributed to Hg^{II} to Hg^{I} reduction [54]. The peak-to-peak separation, ΔE_p, varies with scan rates, showing the quasi-reversible nature of the electron transfer process. On the other hand, in cyclic

Table 3. CV data of 0.1 mmol L^{-1} solutions of **1–4** in CH_3CN/0.1 mol L^{-1} NBu_4ClO_4 at a platinum electrode *vs.* Ag/0.1 mol L^{-1} $AgNO_3$ at different scan rates.

Complex	Scan rate	E_{pa} (V)	i_{pa} (μA)
1	100	0.802	28.40
	200	0.836	40.61
	300	0.884	49.45
	400	0.872	56.81
	500	0.903	62.83
2	100	0.798	58.31
	200	0.806	62.58
	300	0.859	67.54
	400	0.828	77.19
	500	0.882	88.95
3	100	0.832	13.38
	200	0.838	19.60
	300	0.863	24.89
	400	0.835	28.50
	500	0.854	32.05
4	100	0.747	8.41
	200	0.772	11.50
	300	0.786	13.96
	400	0.798	15.59
	500	0.808	17.61

Table 4. CV data of 0.1 mmol L^{-1} solutions of **5–8** in CH_3CN/0.1 mol L^{-1} NBu_4ClO_4 at a platinum electrode *vs.* Ag/0.1 mol L^{-1} $AgNO_3$ at different scan rates.

Complex	Scan rate	E_{pa}/V(1) (i_{pa})/μA	E_{pa}/V(2) (i_{pa})/μA	E_{pc} /V(1) (i_{pc})/μA	E_{pc}/V(2) (i_{pc})/μA	$E^{\circ\prime}$ **(V)(1)**	$E^{\circ\prime}$ **(V)(2)**
5	100	−0.012 (49.10)		−0.521 (−295.00)		−0.266	
	200	−0.023 (69.00)		−0.501 (−341.00)		−0.262	
	300	−0.057 (79.10)		−0.484 (−370.00)		−0.270	
	400	−0.042 (93.70)		−0.472 (−452.00)		−0.257	
	500	−0.086 (111.30)		−0.434 (−509.00)		−0.260	
6	100	−0.004 (67.10)		−0.538 (−330.00)		−0.271	
	200	−0.021 (78.00)		−0.531 (−386.00)		−0.276	
	300	−0.010 (95.10)		−0.506 (−424.00)		−0.258	
	400	−0.052 (102.40)		−0.479 (−451.00)		−0.265	
	500	−0.093 (109.90)		−0.552 (−503.00)		−0.322	
7	100	0.800 (91.50)	1.415 (153.60)	−2.035 (−397.00)	−2.570 (−445.00)	−0.617	−0.577
	200	0.778 (120.60)	1.437 (242.60)	−1.889 (−446.00)	−2.556 (−506.00)	−0.555	−0.559
	300	0.750 (157.00)	1.424 (272.00)	−2.037 (−582.00)	−2.526 (−616.00)	−0.643	−0.551
	400	0.767 (187.00)	1.411 (384.00)	−2.136 (−741.00)	−2.548 (−680.00)	−0.684	−0.568
	500	0.744 (211.00)	1.409 (426.00)	−1.945 (−964.00)	−2.536 (−780.00)	−0.600	−0.563
8	100	0.329 (6.40)	1.099 (16.30)	0.317 (−7.00)	−1.346 (−15.00)	0.323	−0.123
	200	0.325 (10.10)	1.079 (27.70)	0.270 (−26.00)	−1.318 (−18.00)	0.297	−0.119
	300	0.320 (12.60)	1.086 (38.40)	0.259 (−37.00)	−1.328 (−20.00)	0.289	−0.121
	400	0.327 (15.10)	1.093 (50.20)	0.245 (−49.00)	−1.342 (−27.00)	0.286	−0.124
	500	0.312 (16.70)	1.101 (62.80)	0.233 (−61.00)	−1.349 (33.00)	0.272	−0.124

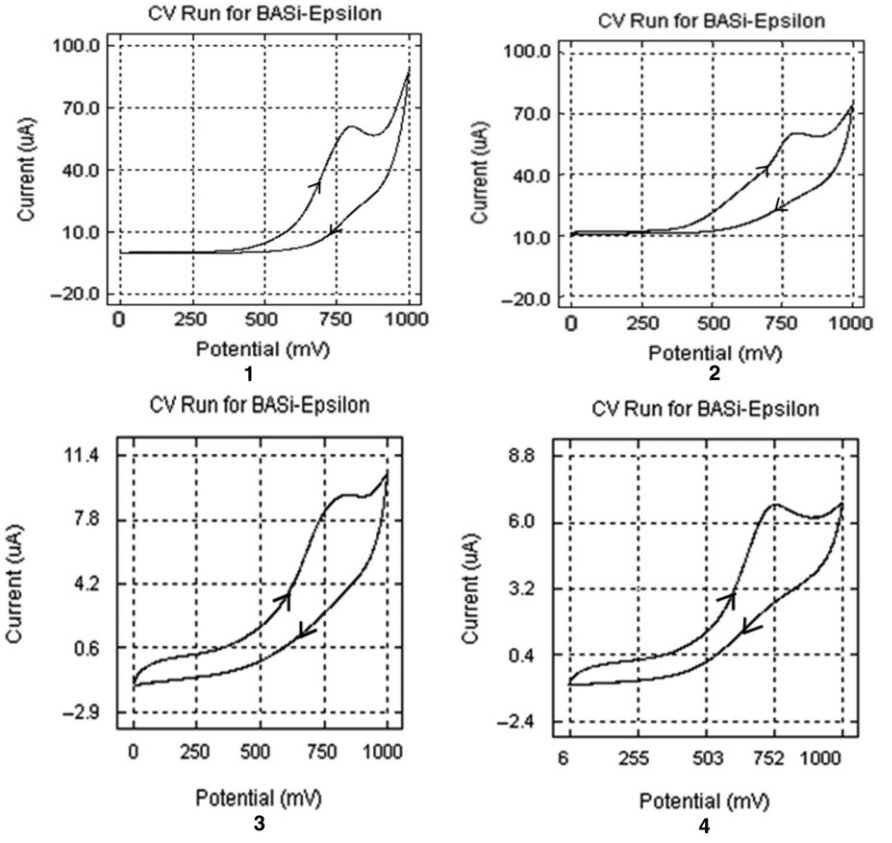

Figure 3. Cyclic voltammograms of 0.1 mmol L^{-1} solutions of **1**–**4** in CH_3CN/0.1 mol L^{-1} NBu_4ClO_4 at platinum electrode *vs.* Ag/0.1 mol L^{-1} $AgNO_3$ at 100 mVs^{-1} scan rate.

voltammograms of **7** and **8** (figure 4), two quasi-reversible waves at $E^{\circ\prime}$ −0.620 V; −0.564 for **7** and 0.293 V; −0.122 V for **8** *versus* Ag/Ag^+ are observed. These electrochemical changes could be assigned to the following electron transfer process:

$$\begin{array}{ccc} Hg^{II}, Hg^{II} & \leftrightarrow & Hg^{II}, Hg^{I} \\ \updownarrow & & \updownarrow \\ Hg^{II}, Hg^{I} & \leftrightarrow & Hg^{I}, Hg^{I}. \end{array}$$

The values of ΔE_p 2776, 3966 mV for **7** and 60, 2428 mV for **8** corresponding to first and second redox couples, respectively, vary with scan rate giving evidence for quasi-reversible nature associated with one-electron reduction. These observations further suggest formation of mono and bimetallic complexes, respectively.

3.5. *DNA-binding properties of 1 and 3*

3.5.1. Electronic absorption spectra. Application of electronic absorption spectroscopy is useful for DNA-binding studies [55–57]. Complex binding with DNA through

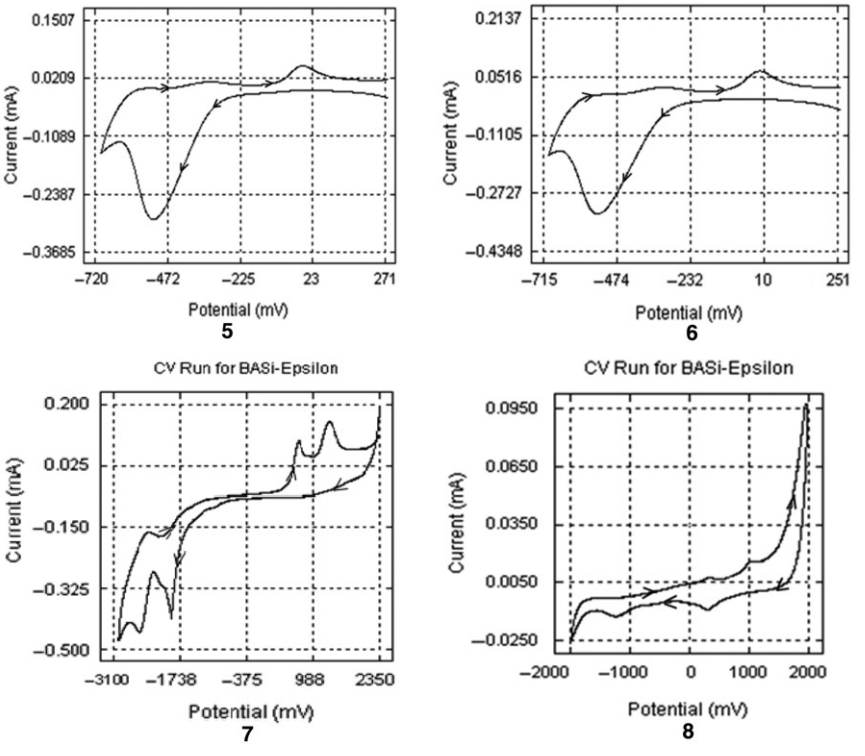

Figure 4. Cyclic voltammograms of 0.1 mmol L^{-1} solutions of **5–8** in CH_3CN/0.1 mol L^{-1} NBu_4ClO_4 at platinum electrode *vs.* Ag/0.1 mol L^{-1} $AgNO_3$ at 100 mVs^{-1} scan rate.

intercalation usually results in hypochromism and bathochromism, due to strong stacking interaction between an aromatic chromophore and the DNA base pairs. The extent of the hypochromism commonly parallels the intercalative binding strength. Absorption spectra of **1** and **3** in the presence and absence of CT-DNA are given figure 5. In the presence of CT-DNA, the absorption band of **1** at 506 nm exhibited hypochromism of about 8.40% and bathochromism of about 4 nm. Complex **3** at 354 nm exhibited hypochromism of about 10.89% and bathochromism of about 3 nm. The values of binding constants K_b of **1** and **3** are 6.1×10^4 $(\text{mol L}^{-1})^{-1}$ and 1.4×10^5 $(\text{mol L}^{-1})^{-1}$, respectively, quite comparable to other Zn(II) complexes reported [58, 59]. These results suggest association of the compounds with DNA, likely through intercalation.

3.5.2. Cyclic voltammetry. CV has been employed to study the interaction of metal complex with DNA to confirm the DNA-bonding modes suggested by the spectral studies [60–62]. Typical CV behavior of **1** in the absence (curve A) and presence (curve B) of CT DNA is shown in figure 6. Summary of voltammetric results for **1** and **3** is given in table 5. Cyclic voltammogram ($\nu = 100$ mVs^{-1}) in the absence of DNA featured the E_{pc} and E_{pa} 0.166 and −0.028 V for **1** and 0.180 and −0.051 V for **3** *versus* Ag/AgCl. The formal potential, $E^{\circ\prime}$ (or voltammetric $E^1/_2$), taken as the average of E_{pc} and E_{pa}, are 0.069 and 0.065 V, respectively. Separation of the anodic and cathodic peak

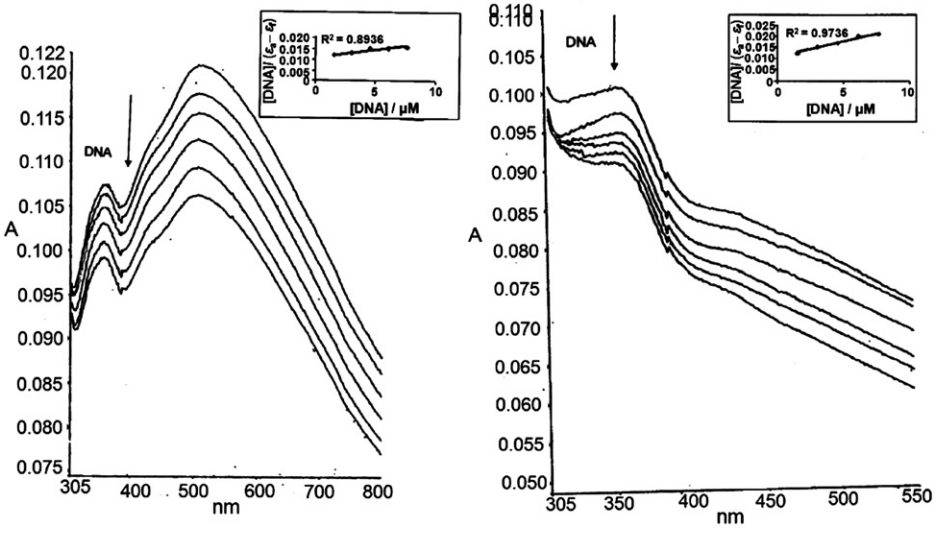

Figure 5. Absorption spectra of **1** and **3** ($30\,\mu mol\,L^{-1}$) at 7.2 pH in the presence of increasing amounts of CT-DNA (0–$80\,\mu mol\,L^{-1}$). Inset: plot of $[DNA]/(\varepsilon_a-\varepsilon_f)$ *vs.* [DNA] for titration of DNA with **1** and **3**. The binding constants K_b of **1** and **3** are 6.1×10^4 $(mol\,L^{-1})^{-1}$ and 1.4×10^5 $(mol\,L^{-1})^{-1}$, respectively.

potentials, ΔE_p, 138 mV for **1** and 129 mV for **3**, indicates quasi-reversible redox processes [63]. In the presence of $30\,\mu mol\,L^{-1}$ DNA, at the same concentration of the complex, the E_{pc} and E_{pa} are 0.188 and −0.016 V for **1** and 0.198 and −0.044 V for **3** *versus* Ag/AgCl. Thus, both anodic and cathodic peak potentials shift to more positive values, implying that **1** and **3** bind to DNA by intercalation [60]. Similar behavior was also observed while increasing DNA concentration and scan speed. In addition to changes in formal potential upon addition of DNA, the voltammetric current also decreases. The decrease in the voltammetric current and the shift of the peak potential in the presence of CT DNA can be attributed to diffusion of the metal complex bound to the large, slowly diffusing DNA molecule.

4. Conclusion

Reactions of $\mathbf{L^1H}$, $\mathbf{L^2H}$, $\mathbf{L^3H}$, and $\mathbf{L^4H}$ with $ZnCl_2$ led to the formation of bimetallic complexes with partial hydrolysis of proligand liberating phenylchalcogeno(alkyl)aminehydrochloride. Two molecules of partially hydrolyzed ligand are coordinated to two Zn(II) ions through imino N, phenolic O, and benzoyl O with phenolic O bridging two metals, leaving the chalcogen (Se and Te) uncoordinated. Each Zn(II) is five coordinate with square-pyramidal geometry with O_3NCl coordination sphere. The reactions of $\mathbf{L^1H}$ and $\mathbf{L^2H}$ with $HgBr_2$ yielded the 14- and 16-membered monometallic metallamacrocyclic complexes **5** and **6** through coordination of mercury with selenium only, without undergoing hydrolysis of proligand molecules. With $\mathbf{L^3H}$ and $\mathbf{L^4H}$ 16- and 18-membered bimetallic metallamacrocyclic complexes **7** and **8** resulted through coordination of mercury with tellurium. The binding of **1** and **3** with CT-DNA were

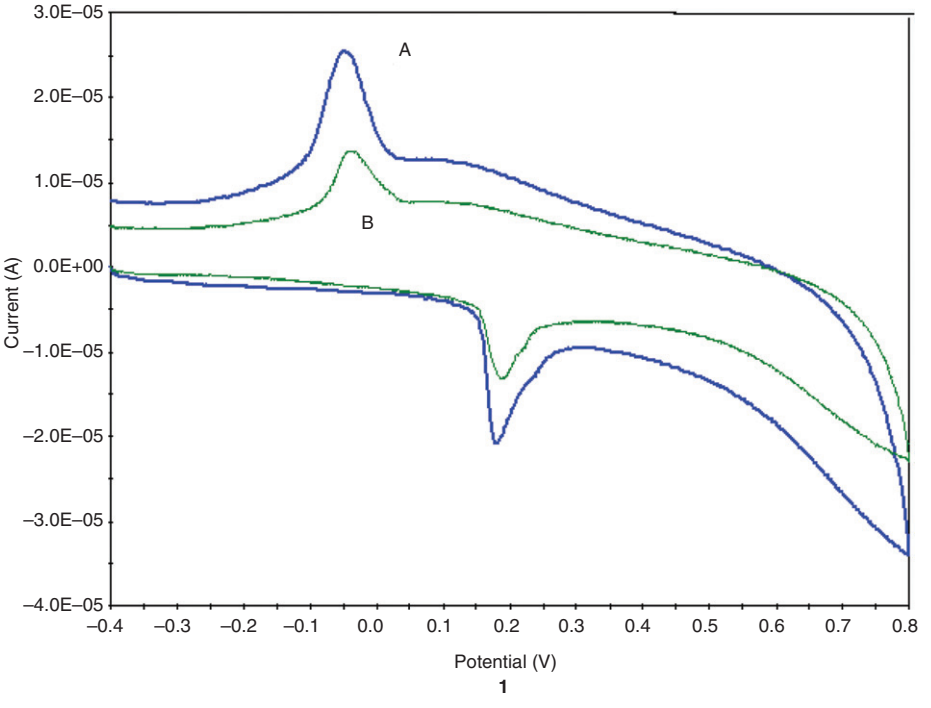

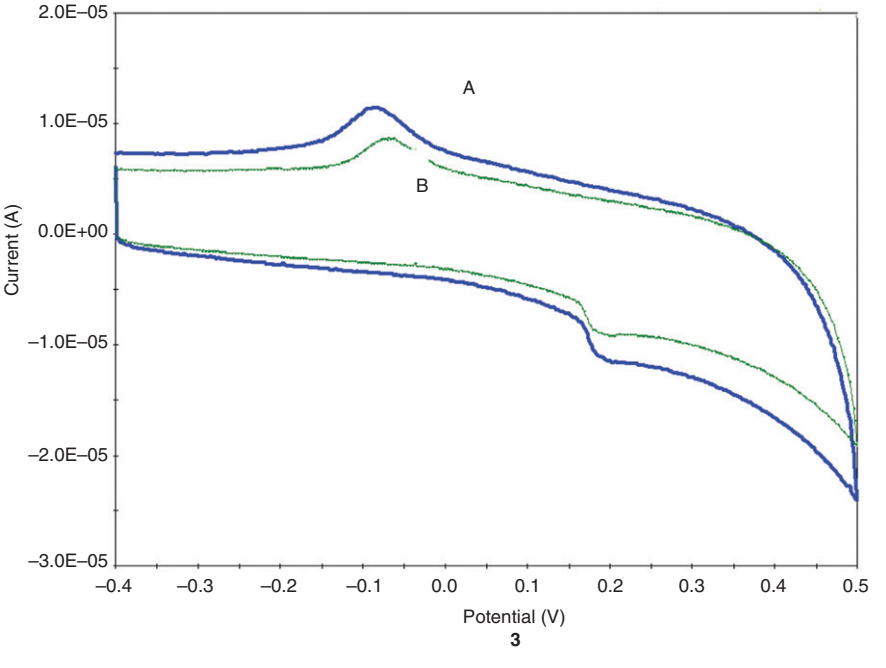

Figure 6. Cyclic voltammograms of **1** and **3** (30 μmol L^{-1}) in the absence (A) and presence (B) of CT DNA (30 μmol L^{-1}) in 50 mmol L^{-1} NaCl, 5 mmol L^{-1} Tris, pH 7.2. Scan rate, 200 mV s^{-1}.

Table 5. CV behavior of **1** and **3** in the presence of CT DNA.

Complex	Scan rate ($mV\,s^{-1}$)	R	E_{pa} /V (i_{pa}) (μA)	E_{pc}/V (i_{pc}) (μA)	ΔE_p (mV)	$E^{\circ\prime}$ (V)
1	100	0	−0.028 (16.16)	0.166 (−17.7)	138	0.069
		30	−0.016 (9.81)	0.188 (−20.0)	172	0.086
	200	0	−0.054 (25.5)	0.178 (−22.3)	124	0.062
		30	−0.048 (14.18)	0.214 (−24.3)	166	0.083
	300	0	−0.068 (34.85)	0.190 (−28.5)	122	0.061
		30	−0.061 (21.2)	0.220 (−29.5)	159	0.079
	400	0	−0.078 (36.68)	0.198 (−31.2)	120	0.060
		30	−0.074 (26.92)	0.230 (−35.2)	156	0.078
3	100	0	−0.051 (6.54)	0.180 (−4.30)	129	0.065
		30	−0.044 (5.43)	0.188 (−5.87)	144	0.072
		60	−0.040 (4.4)	0.202 (−6.15)	162	0.081
	200	0	−0.076 (10.2)	0.185 (−7.2)	109	0.054
		30	−0.063 (8.64)	0.194 (−8.92)	131	0.065
		60	−0.056 (7.41)	0.208 (−10.3)	152	0.076
	300	0	−0.087 (14.5)	0.192 (−9.8)	105	0.052
		30	−0.079 (11.4)	0.198 (−10.3)	119	0.059
		60	−0.072 (9.52)	0.215 (−12.32)	143	0.071
	400	0	−0.096 (16.6)	0.197 (−13.6)	101	0.051
		30	−0.086 (13.2)	0.208 (−14.3)	122	0.061
		60	−0.083 (12.7)	0.222 (−16.81)	139	0.069

$\Delta E_p = (E_{pa} - E_{pc})$; $E^{\circ\prime} = ½\ (E_{pa} + E_{pc})$; Complex 30 μmol L^{-1}; R = [DNA]/[Complex].
Supporting electrolyte, 50 mmol L^{-1} NaCl + 5 mmol L^{-1} Tris, pH 7.2; Working electrode: Pt; Reference electrode: Ag/AgCl.

studied by electronic absorption spectra and CV, suggesting they bind with the helix of CT-DNA by intercalation. The intrinsic binding constants K_b obtained from spectral titration are comparable to other Zn(II) complexes reported in the literature.

Supplementary material

CCDC 828990 contains the supplementary crystallographic data for **1**. These data can be obtained free of charge from Cambridge Crystallographic Data Centre *via* www.ccdc.cam.ac.uk/data_request/cif or from the Cambridge Crystallographic Data Centre, 12 Union Road, Cambridge CB2 1EZ, UK; Fax: (+44) 123-336-033 or E-mail: deposit@ccdc.cam.ac.uk.

Acknowledgments

We are grateful to DRDO, New Delhi for the financial assistance and for the award of fellowship to AKA. We thank Prof. B.L. Khandelwal, DIMAT, Raipur and Dr J.D. Smith, University of Sussex, UK for useful discussion, and Prof. Sandeep Verma, IIT Kanpur for providing mass spectra. We also thank the reviewers for their constructive suggestions.

References

[1] C. Santi, S. Santoro, B. Battistelli. *Curr. Org. Chem.*, **14**, 2442 (2010).
[2] Y. Nishibayashi, S. Uemura. *Top. Curr. Chem.*, **208**, 235 (2000).
[3] P.A. Chaloner. *J. Organomet. Chem.*, **359**, C28 (1989).
[4] T. Sohn, M.J. Kim, D. Kim. *J. Am. Chem. Soc.*, **132**, 12226 (2010).
[5] B. Kim, M. Lee, M.J. Kim, H. Lee, S. Kim, D. Kim, M. Koh, S.B. Park, K.J. Shin. *J. Am. Chem. Soc.*, **130**, 16807 (2008).
[6] A.L. Braga, D.S. Luedtke, F. Vargas, R.C. Braga. *Chem. Inform.*, **37**, 1453 (2006).
[7] A. Molter, F. Mohr. *Coord. Chem. Rev.*, **254**, 19 (2010).
[8] D.K. Dutta, B. Deb. *Coord. Chem. Rev.*, **255**, 1686 (2011).
[9] W. Levason, S.D. Orchard, G. Reid. *Coord. Chem. Rev.*, **225**, 159 (2002).
[10] R.L. Davidovich, V. Stavila, K.H. Whitmire. *Coord. Chem. Rev.*, **254**, 2193 (2010).
[11] G. Mugesh, W.W. du Mont, H. Sies. *Chem. Rev.*, **101**, 2125 (2001).
[12] A. Wendel. *Selenium in Biology and Medicine*, 1st Edn, Springer-Verlag, Berlin (1989).
[13] K. Sarma, G. Mugesh. *Org. Biomol. Chem.*, **6**, 965 (2008).
[14] L. Seminario-Vidal, C. van Heusden, G. Mugesh, E.R. Lazarowski. *Purinergic Signal.*, **6**, 383 (2011).
[15] Z. Ding, S.K. Bux, D.J. King, F.L. Chang, T.-H. Chen, S.-C. Huang, R.B. Kaner. *J. Mater. Chem.*, **19**, 2588 (2009).
[16] R.K. Chapek, K. Lambert, D. Dorfs, P.F. Smet, D. Poelman, A. Eychmuller, Z. Hens. *Chem. Mater.*, **21**, 1743 (2009).
[17] E.A. Turner, H. Rosner, Y. Huang, J.F. Corrigan. *J. Phys. Chem. C*, **111**, 7319 (2007).
[18] V. Protasenko, D. Bacinello, M. Kuno. *J. Phys. Chem. B*, **110**, 25322 (2006).
[19] A. Molter, F. Mohr. *Coord. Chem. Rev.*, **254**, 19 (2010).
[20] P.D. Boyle, S.M. Godfrey. *Coord. Chem. Rev.*, **223**, 265 (2001).
[21] T. Chivers, R.W. Hilts. *Coord. Chem. Rev.*, **13**, 201 (1994).
[22] M.A. Malik, M. Afzaal, P. O'Brien. *Chem. Rev.*, **110**, 4417 (2010).
[23] W.-S. Chang, Y.-F. Lin, B. Sarkar, Y.-M. Chang, L.-K. Liu, C.W. Liu. *J. Chem. Soc., Dalton Trans.*, 2821 (2010).
[24] K.-H. Low, C.-H. Li, V.A.L. Roy, S.S.-Y. Chui, S.L.-F. Chan, C.-M. Che. *Chem. Sci.*, **1**, 515 (2010).
[25] A. Panneerselvam, M.A. Malik, M. Afzaal, P. O'Brien, M. Helliwell. *J. Am. Chem. Soc.*, **130**, 2420 (2008).
[26] K.P. Bhabak, G. Mugesh. *Acc. Chem. Res.*, **43**, 1408 (2010).
[27] K.P. Bhabak, G. Mugesh. *Inorg. Chem.*, **48**, 2449 (2009).
[28] M.J. Bowers II, J.R. McBride, S.J. Rosenthal. *J. Am. Chem. Soc.*, **127**, 15378 (2005).
[29] V.L. Colvin, M.C. Schlamp, A.P. Alivisatos. *Nature*, **370**, 354 (1994).
[30] T.-P. Hsieh, C.-C. Chuang, C.-S. Wu, J.-C. Chang, J.-W. Guo, W.-C. Chen. *Solid-State Electron.*, **56**, 175 (2011).
[31] M. Afzaal, P. O'Brien. *J. Mater. Chem.*, **16**, 1597 (2006).
[32] T. Niu, Y. Gu, J. Huang. *J. Mater. Chem.*, **21**, 651 (2011).
[33] D.L. Klein, R. Roth, A.K.L. Lim, A.P. Alivisatos, P.L. McEuen. *Nature*, **389**, 699 (1997).
[34] V.K. Verma, A.K. Asatkar, T.A. Jain, S.K. Tripathi, R. Singh, P.B. Hitchcock, S. Nigam, S.K. Gupta. *Polyhedron*, **28**, 2591 (2009).
[35] S. Nair, V.K. Verma, C.S. Verma, T.A. Jain, S.K. Tripathi, R. Singh, S.K. Gupta, R.J. Butcher. *J. Coord. Chem.*, **63**, 4088 (2010).
[36] V.W.L.F. Armarego, D.D. Perrin. *Purification of Laboratory Chemicals*, 4th Edn, Pergamon Press, Oxford (1997).
[37] G.M. Sheldrick. *Acta Crystallogr., Sect. A*, **64**, 112 (2008).
[38] Oxford Diffraction. *CrysAlis PRO and CrysAlis RED*, Oxford Diffraction Ltd., Abingdon, England (2007).
[39] J.J. Marmur. *J. Mol. Biol.*, **3**, 208 (1961).
[40] M.F. Reichmann, S.A. Rice, C.A. Thomas, P.J. Doty. *J. Am. Chem. Soc.*, **76**, 3047 (1954).
[41] A. Wolfe, G.H. Shimer, T. Meehan. *Biochemistry*, **26**, 6392 (1987).
[42] K. Nakamoto. *Infrared and Raman Spectra of Inorganic and Coordination Compounds*, 5th Edn, Wiley, New York (1997).
[43] A.T. Çolak, O.Z. Yeşilel, O. Büyükgüngör. *Polyhedron*, **29**, 2127 (2010).
[44] J. Klingele, G. Steinfeld, M.H. Klingele. *Transition Met. Chem.*, **35**, 65 (2010).
[45] T.P. Stanojkovic, D. Kovala-Demertzi, A. Primikyri, I. Garcia-Santos, A. Castineiras, Z. Juranic, M.A. Demertzis. *J. Inorg. Biochem.*, **104**, 467 (2010).
[46] E. Almaraz, W.S. Foley, J.A. Denny, J.H. Reibenspies, M.L. Golden, M.Y. Darensbourg. *Inorg. Chem.*, **48**, 5288 (2009).
[47] M. Poyraz, M. Sar, A. Guney, F. Demirci, S. Demirayak, E. Sahin. *J. Coord. Chem.*, **61**, 3276 (2008).
[48] C. Sudbrake, H. Vahrenkamp. *Inorg. Chim. Acta*, **318**, 23 (2001).

[49] Y. Sugiura, Y. Tamai, H. Tanaka. *Bioinorg. Chem.*, **9**, 167 (1978).
[50] G. Mugesh, H.B. Singh, R.J. Butcher. *J. Organomet. Chem.*, **577**, 243 (1999).
[51] S.D. Apte, S.S. Zade, H.B. Singh, R.J. Butcher. *Organometallics*, **22**, 5473 (2003).
[52] G. Mugesh, H.B. Singh, R.J. Butcher. *Inorg. Chem.*, **44**, 147 (2005).
[53] B. Dutta, P. Bag, U. Florke, K. Nag. *Inorg. Chem.*, **44**, 147 (2005).
[54] H.-R. Wen, J.-L. Zuo, T.A. Scott, H.-C. Zhou, X.-Z. You. *Polyhedron*, **24**, 671 (2005).
[55] J.K. Barton, A.L. Raphael. *J. Am. Chem. Soc.*, **106**, 2172 (1984).
[56] T.M. Kelly, A.B. Tossi, D.J. McConnell, T.C. Streaks. *Nucleic Acids Res.*, **13**, 6017 (1985).
[57] S.A. Tysoe, R.J. Morgan, A.D. Baker, T.C. Streaks. *J. Phys. Chem.*, **97**, 1707 (1993).
[58] N. Raman, A. Sakthivel, R. Jeyamurugan. *J. Coord. Chem.*, **63**, 1080 (2010).
[59] P. Zhao, J.W. Huang, L.N. Ji. *J. Coord. Chem.*, **64**, 1977 (2011).
[60] M.T. Carter, M. Rodriguez, A.J. Bard. *J. Am. Chem. Soc.*, **111**, 8901 (1989).
[61] M.T. Carter, A.J. Bard. *J. Am. Chem. Soc.*, **109**, 7528 (1987).
[62] D.H. Johnston, R.C. Glasgow, H.H. Thorp. *J. Am. Chem. Soc.*, **117**, 8933 (1995).
[63] P. Zanello. *Inorganic Electrochemistry, Theory, Practice and Application*, Vol. 314, The Royal Society of Chemistry, Cambridge (2003).